PHARMACIA

Pharmacia 69(3): 855–864
DOI 10.3897/pharmacia.69.e91057

Research Article

Green synthesis of metronidazole or clindamycin-loaded hexagonal zinc oxide nanoparticles from *Ziziphus* extracts and its antibacterial activity

Saba Abdulmunem Habeeb[1], Asmaa H. Hammadi[2], Dhulfiqar Abed[1], Lena Fadhil Al-Jibouri[3]

1 *Department of Pharmaceutical Chemistry, College of Pharmacy, University of Babylon, Babylon 51001, Iraq*
2 *Department of Pharmaceutics, College of Pharmacy, University of Babylon, Babylon 51001, Iraq*
3 *Department of Clinical Laboratory Sciences, College of Pharmacy, University of Babylon, Babylon 51001, Iraq*

Corresponding author: Dhulfiqar Abed (phar.dhoalfaqar.ali@uobabylon.edu.iq)

Received 30 July 2022 ♦ **Accepted** 17 August 2022 ♦ **Published** 14 September 2022

Citation: Habeeb SA, Hammadi AH, Abed D, Al-Jibouri LF (2022) Green synthesis of metronidazole or clindamycin-loaded hexagonal zinc oxide nanoparticles from *Ziziphus* extracts and its antibacterial activity. Pharmacia 69(3): 855–864. https://doi.org/10.3897/pharmacia.69.e91057

Abstract

Green chemistry has become a fruitful approach for the synthesis of semiconductors and nanoparticles with various applications. Herein, we synthesized ZnO hexagonal nanoparticles (HNPs) by green precipitation method using fresh local *Ziziphus* leaf extract (Rhamnaceae) with a heating range of 60–80 in an alkaline medium. It was calcinated on a furnace at 500 °C for 2 h. to get a very fine and homogeneous pale-yellow powder which is then loaded with either metronidazole or clindamycin. The physical characterizations of the particles' morphology, size, and purity were measured using the Scanning electron microscope, UV-spectroscopy, and the Fourier transform infrared spectroscope. The size of ZnO nanoparticles (44.63 nm) was measured using scanning electron microscopy (SEM), and the mean crystal size of the precursor (17.37 nm) was measured using X-ray diffraction methods (XRD). The antibacterial activity of these particles was measured against Staphylococcus aureus bacterial strains and analyzed using a "well-diffusion technique" which revealed that metronidazole or clindamycin-containing ZnO nanoparticles showed good bactericidal activity.

Keywords

ZnO (HNPs), GS, *Ziziphus* leaf extract, drug delivery, Antibacterial activity

1. Introduction

Nanotechnology is an emergent new research field that deals with the synthesis of nanostructures and nanoparticles (NPs) and their use in numerous fields including pharmaceutics, electrical chemistry, biomedical technologies, catalysis, makeups, sensors, nutrition technology, health care, fabric industry, mechanics, physical optics, microelectronics, space engineering, and energy discipline, etc. (Ahmed et al. 2017). Nanotechnology comprises the production of molecules at a nano-measure under a controlled milieu. The NPs have various physical and chemical alterations in their characteristics such as biomechanical features, electrical conductivity, optical absorptive activity, melting degree, and catalysis activity compared with large substances with a similar chemical structure (Perveen et al. 2020). The novel features of NPs are extensively arranged for several applications in biomedicine, makeups, medical devices, as well as environmental remediation (Jamdagni et al. 2016). NPs are also known as the "wonder of modern medicine" owing to its characteristic properties. Several physical and biochemical approaches

Copyright *Habeeb SA et al.* This is an open access article distributed under the terms of the Creative Commons Attribution License (CC-BY 4.0), which permits unrestricted use, distribution, and reproduction in any medium, provided the original author and source are credited.

PENSOFT

are introduced for the production of NPs, in which several unsafe and very toxic compounds are applied (Siddiqi et al. 2018). Hence, a suitable substitute is essential, which could be attained by green synthesis (GS). GS of NP is a common eco-friendly method (Kolekar et al. 2013; Jamdagni et al 2016), using plants extract is due to numerous advantages, including better products and worth of NPs obtained, easiness of process and control, safety, the richness of resources, and cost-effective (Matussin et al. 2020; Rahman et al. 2021). The GS act as a good substitute for physical and chemical procedures due to its cheap and safe substrates. Numerous existing reports in the preceding years, undoubtedly point to the significant antimicrobial action of oxides of inorganic metals like Zinc oxide, MgO, TiO2, CaO, CeO_2, and SiO2. Especially, ZnO, TiO_2, CaO, and MgO are of precise concern as they are not just steady under harsh method circumstances, but as well are regarded as safe constituents (Jamdagni et al. 2016). Zinc oxide (ZnO) is a safe and low-cost compound with an extensive "band gap energy" (~3.2 eV) among several kinds of semiconductors (Ahmed et al. 2017; Rahman et al. 2021). ZnO has many extraordinary features and is used in diverse applications, like photocatalysts, dyes, biosensors solar cells, sun cream, antioxidants, and antimicrobial products (Siddiqi et al. 2018). ZnO-NPs are the utmost projecting ones due to their exclusive optical and chemical performances being regulated by morphology. ZnO white powder is water insoluble. The flame retardants, iron-containing ferrites, batteries, nutrition, colorings, sealants, creams, glues, emollients, plastics, elastic, adhesive, glass, and ceramic wares employ ZnO powders as an improver (Ahmed et al. 2017; Qureshi et al. 2019; Perveen et al. 2020). As well, because of its high antimicrobial action, ZnO exhibits exceptional activity against a wide range of microbes besides being safe and biocompatible with body cells. For instance, synthesized ZnO leaf extracts of *Glycosmis pentaphylla* exposed extraordinary antibacterial effect against Gram-positive bacteria (*B. cereus* and *S. aureus*), Gram-negative bacteria (*S. dysenteriae* and *S. paratyphi*) and fungi (*C. Albicans* and *A. niger*) (Vijayakumar et al. 2018). *Staphylococcus aureus* is a gram-positive bacterium, normally detected in humans. In some instances, it turns into a real problem in the course of infection control. Due to the suitability of admission and the country's compact inhabitants, cases with *S. aureus* infections are persistently ill or have been newly treated for diverse causes (Roy et al. 2013; Haque et al. 2018; Vadekeetil et al. 2019). It is difficult to differentiate nosocomial from community-acquired infections. Physicians have directed investigation on the molecular bases of vancomycin-resistant *S. aureus*, to overcome this issue (Tong et al. 2015; Mohamed et al. 2016; Peterson et al. 2018).

The antibacterial effects of ZnO NPs may be due to the intrinsic toxicity of metal particles. The loss of bacterial integrity may be related to the interaction between the cell wall and the ZnO NPs. Furthermore, ZnO NPs can cause environmental changes in the bacteria, (ROS production) which can induce cellular damage (da Silva et al. 2019). The possible mechanisms of ZnO NPs toxicity are illustrated schematically in Fig. 1.

Osteomyelitis is a multi-bacterial infection and in around 80% of cases caused by *S. aureus* bacteria. The present surgical therapy of osteomyelitis is a combination of antibiotics and bone cement that is set in into the site of bone marrow infection. Nevertheless, inadequate drugs exist to treat antimicrobial-resistant strains. Thus, drug companies have tried to develop recent antibacterial agents (Rizzello et al. 2014; Abd EL-Tawab et al. 2018; Kung et al. 2020). Recently, one of the approaches to resolve antibiotic resistance is the use of metal NPs and their oxides.(Hammadi et al. 2020; Abdelraheem et al. 2021).

Zizphus spina Christ (Rhamnaceae)

It is one of the Iraqi perennial spikey plants, and it distributes from the central to the south of Iraq because of the increased temperature and moisture (Alnehia et al. 2022). The tree itself has medical characteristics like antimicrobial, antidiarrheal, antioxidant, and anti-diabetes (Dhanalekshmi et al. 2022). The leaves of this plant have been utilized as wound dressings, bronchial asthma, and fever remedies. Phytochemical analyses of the leaf extracts (aqueous and methanolic extract) were performed and revealed the presence of saponins, alkaloids, flavonoids, tannins, and polyphenols (Arif et al. 2022). Current work was performed to evaluate the effect of "microbial catalyst" on the morphology of ZnO- NPs using the green synthesis technique. In addition, the structural features of the synthesized ZnO-NPs were measured, as well as their antimicrobial activity.

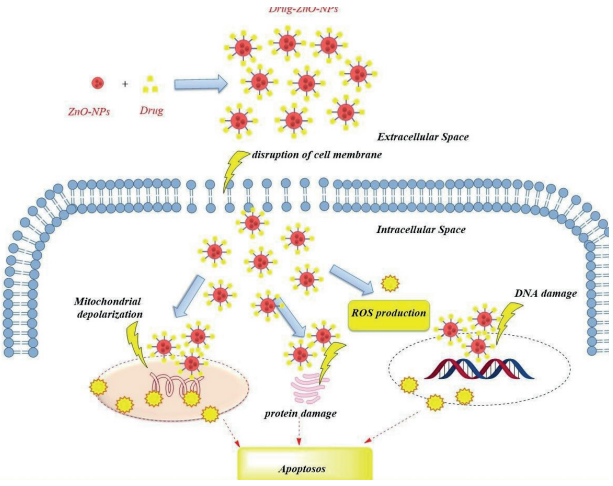

Figure 1. Schematic diagram of the proposed mechanisms of ZnO NPs antibacterial effects.

2. Experiment setup

2.1. Chemicals section

Zinc nitrate $ZnNO_3$, $6(H_2O)$, NaOH, and ethanol utilized in the study were of the analytical score and were provided from the markets. Clindamycin and metronidazole were

purchased from Wuhan Fortuna Chemical Co. (China). All glassware was cleaned with sterilized distilled water (DW) and then dried out in an electrical oven before its use.

2.2. Preparation of leaf extract

Fifty grams of fresh *Ziziphus* buckthorn leaves were collected and then washed away with tap water and then with deionized water frequently to get rid of dust and impurities, and the leaves were let dry in the air while maintaining the freshness of the leaves. Then, after adding 500 cc deionized water, the leaves were crushed with a high-speed blender, and then the solution was filtered using filter papers several to separate the leaf residues from the extract. The extract is a homogeneous dark green solution that is denser than water, free of sediment, and kept at 4 °C until compound fabrication.

2.3. Green Synthesis of ZnO (HNPs)

About 200 g of prepared plant extract (B) was taken to heat at 60–80 °C on a hot plate with stirring for 2 hours, and then 10 gm of zinc nitrate was added to the hot solution with rapid and stable stirring. Once the zinc nitrate was completely dissolved, a few drops of sodium hydroxide was added to maintain the basic condition. The mixture was stirred at room temperature for about eight hours until the greenish liquid slowly started to fade with the appearance of yellow-colored suspension followed by the formation of a pale-yellow precipitate. The precipitate was collected with filter paper and cleaned with tap water and ethanol to eliminate insoluble zinc nitrate and other impurities. The precipitate was dried in an oven for about 12 hrs at 80 °C, and lastly calcining for 2 hrs at 500 °C ovens. The steps used for the synthesis of hexagonal Zinc Oxide Nanoparticles (ZnO-HNPs) are illustrated schematically in Fig. 2.

2.4. Drug loading on ZnO (HNPs)

To load the drug into hexagonal ZnO-nanostructures, zinc oxide (HNPs) was dissolved in solutions of 100 milliliters of DW at three concentrations (0.1, 0.5, and 1%). Then, 40 mg of either clindamycin or metronidazole was added to the three solutions before stirring by a magnetic stirrer at 600 rpm for a minimum of five hours at room temperature. At that point, the solutions were left overnight, and then centrifugated at 5×10^3 rpm for 10 minutes to get yellow precipitate. (Palanikumar et al. 2013)

2.5. Biology section

The fresh *Ziziphus leaf* was obtained from the garden of Al-Hilla city. To investigate the antibacterial efficacy of gram-positive *S. aureus* and gram-negative *P. aeruginosa*, "the agar well diffusion" technique was selected, and cultured in a media of nutrient agar. After 24 hours, one hundred microliters of old mature cultured media were swabbed using the L-shaped rod on the medium. The wells were made with a sterile cork tool (6 mm). In current study, ZnO-HNPs concentrations in triplicate had been used (0.1%, 0.5% and 1%). Each concentration was utilized separately with metronidazole or with clindamycin. "Zone of inhibition" (ZOI) was calculated in millimeters. In each Petri dish, three wells were prepared and fifty µl of each specified concentration was added individually (Chikkanna et al. 2019).

3. Results and discussion

3.1. Morphology and size

3.1.1. SEM

Fig. 3a, b represents the SEM image of ZnO-HNPs. It indicates the formation of nano-grained zinc oxide with a well-faceted hexangular hollow prism outline due to the highly crystallized quality of the samples with free surfaces and well-formed grain margins. It has been lately verified that the physical characteristics of pure zinc oxide nano-grains are based on the existence of defects like interphase boundaries, grain margins, and free surfaces (Bitenc et al. 2010). The NPs produced due to the breakdown has the outline of the hexangular hollow prism (Fig. 3). High porosity is a characteristic of this nano-grained ZnO.

Fig. 4 displays the width distribution of the formed ZnO-HNPs, which were measured with image-j software (Malode et al. 2020; Zoubir et al. 2021). The ZnO-HNPs appeared to spread over the whole surface with a mean size of about 44.63 nm, which indicates the high porosity of constructed electrode used in the technique.

Fig. 5 displays the SEM morphology of ZnO-HNPs of clindamycin. This suggests that the concentrations of the drug have appropriate viscosity to synthesize NPs.

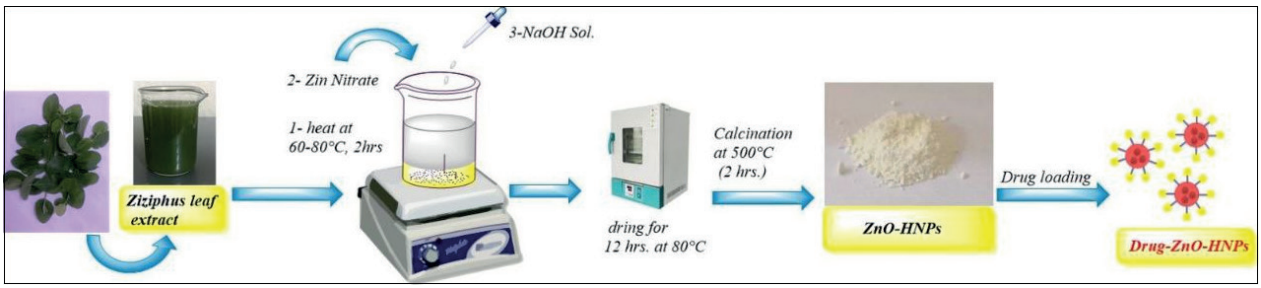

Figure 2. Schematic diagram of the steps used for synthesis of Drug-loaded hexagonal Zinc Oxide Nanoparticles (ZnO-HNPs).

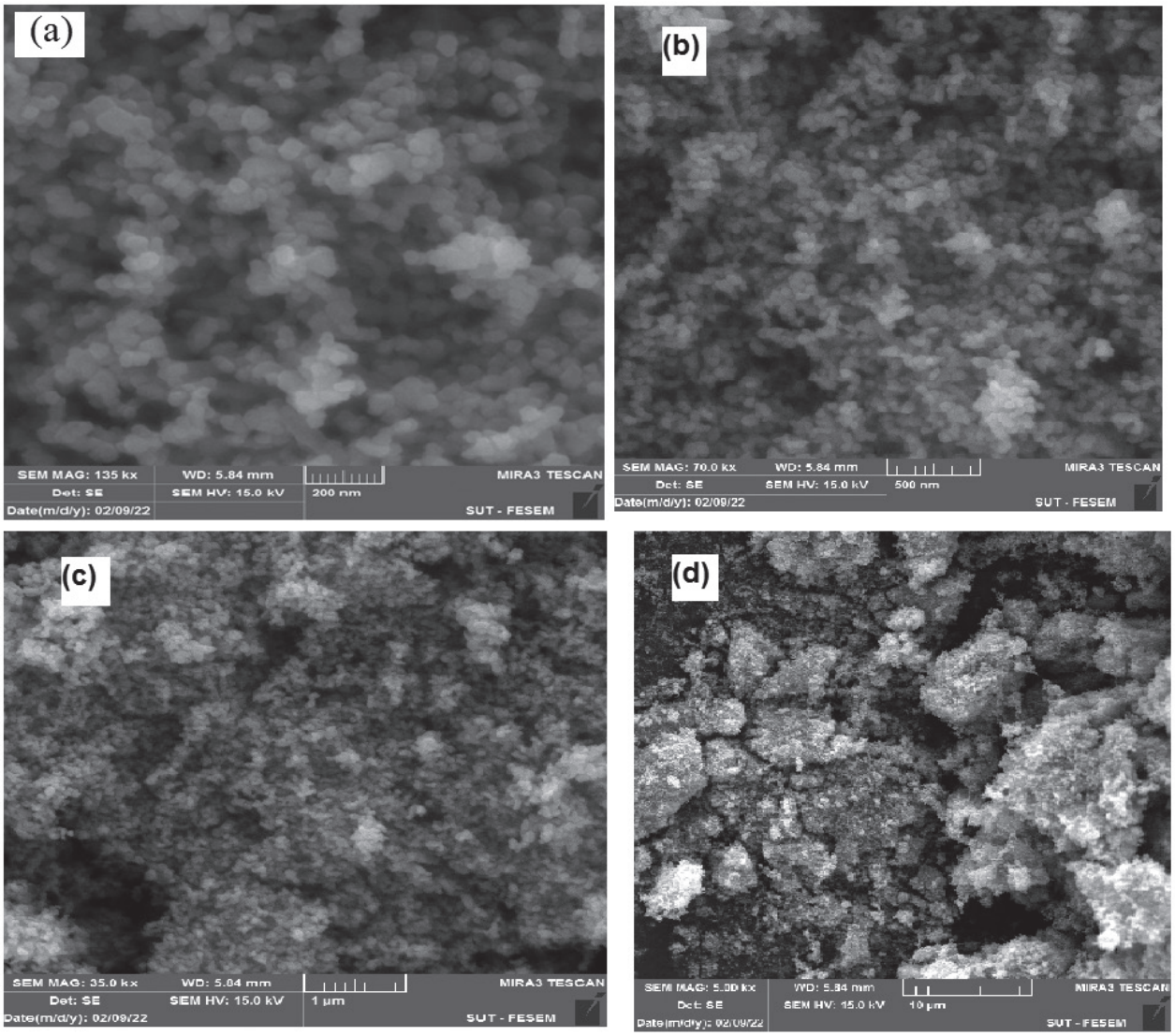

Figure 3. SEM micrograph of zinc oxide hexagon nanostructures (**a**) 200 nm, (**b**) 500 nm, (**c**) 1 µm and (**d**) 10 µm.

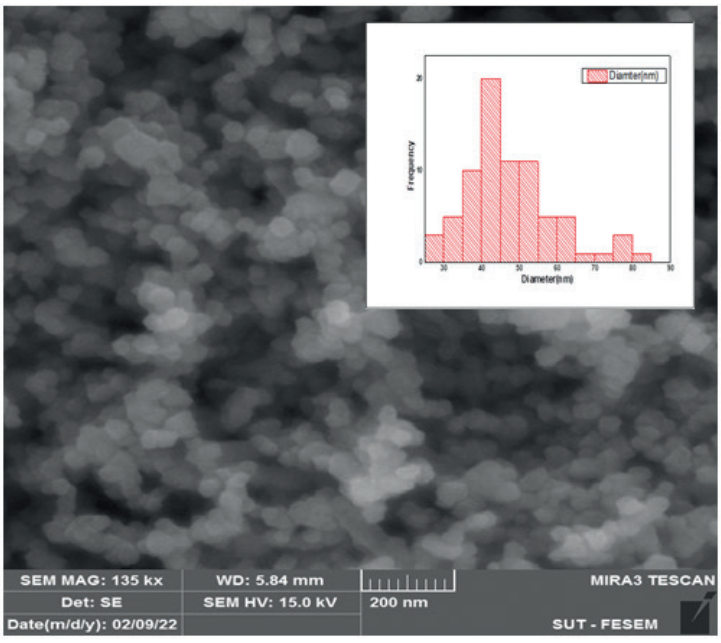

Figure 4. Histogram show the distribution of ZnO-HNPs according to their diameter .

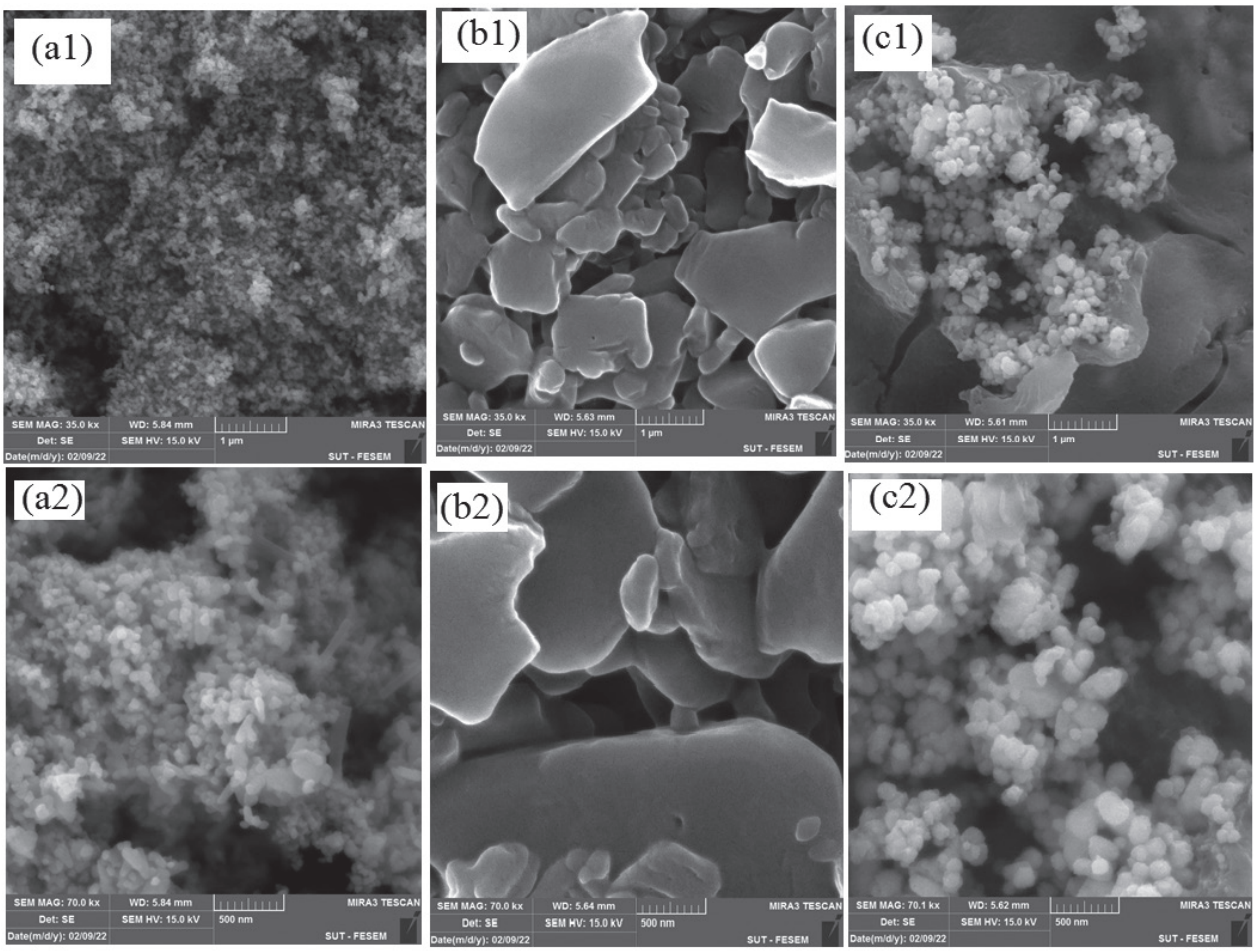

Figure 5. SEM micro images of (**a**) ZnO-HNPs, (**b**) clindamycin alone, (**c**) clindamycin/ZnO-HNPs, (**1**) 1 μm, and (**2**) 500 μm.

Consequently, constant and regular NPs were formed effectively. This indicates that adding clindamycin results in an increased diameter of the ZnO-HNPs.

Fig. 6 exhibits the SEM imaging of the metronidazole-ZnO-HNPs. The surface shape of metronidazole has altered after being loaded with ZnO-HNPs. As we can see in Fig. 6c, the NPs manifested as granules with a light color which are evenly spread over the surface of metronidazole. In Fig. 6c, we can see the SEM micrograph of the ZnO-HNPs after reaction with metronidazole. The morphology of these HNPs was altered completely, and the greatest available holes and pores on the surface of ZnO-HNPs were occupied by metronidazole particles. When comparing Fig. 6a, b with Fig. 6c, we can see the significant change in the morphology of metronidazole-ZnO-HNPs.

3.1.2. X-ray diffraction pattern of ZnO (XRD)

The crystalline character of ZnO-NPs was measured by XRD and the pattern displays peaks at "[31.6, 34.2, 36.2, 47.35, 56.41,62.55, 66.17, 67.71, 68.96, 72.3, and 77.78°]" similar to lattice planes "[(100), (002), (101), (102), (110), (103), (200), (112), (201), (004) and (202)]", respectively. No XRD peaks associated with impurities and/or any intermediary ingredients were detected, which further indicates the purity of synthesized ZnO hexagons powder (Ada et al. 2008). As we can see in Fig. 7, the obtained sharp and narrow diffraction peaks indicate the formation of ZnO-HNPs with optimum crystallinity and size. The crystallite size of the formed ZnO-HPNs sample was estimated to be 17.37 nm and measured with the "Debye-Scherrer formula" (Sornalatha et al. 2014; Scherrer 1918):

$$D = (0.89\,\lambda) / (\beta \cos \theta)$$

3.1.3. UV-visible spectrophotometric analysis

The spectrophotometric absorptive pattern normally depends on the variables like the temperature, size, and shapes of the synthesized nanostructures (Moghri et al. 2012). The UV–vis absorption of the ZnO-NPs is correlated with their size. The material surface and interface are important in the process of light absorption. The UV–Vis spectrum of the ZnO-HPNs was measured in deionized water. Fig. 8 demonstrates the UV–Vis spectrum of ZnO-HNPs calculated at room temperature. Broadband can be observed at 367 nm (3.29 eV), which was similar to the bandgap of zinc oxide "1s–1s electron transition" (3.37eV) (16).

3.1.4. The Fourier transform infrared spectroscopy (FTIR) spectrum

The ZnO-HNPs FTIR spectrum lies in the range of 4000–400 cm^{-1} and was presented in Fig 9. The band sited within

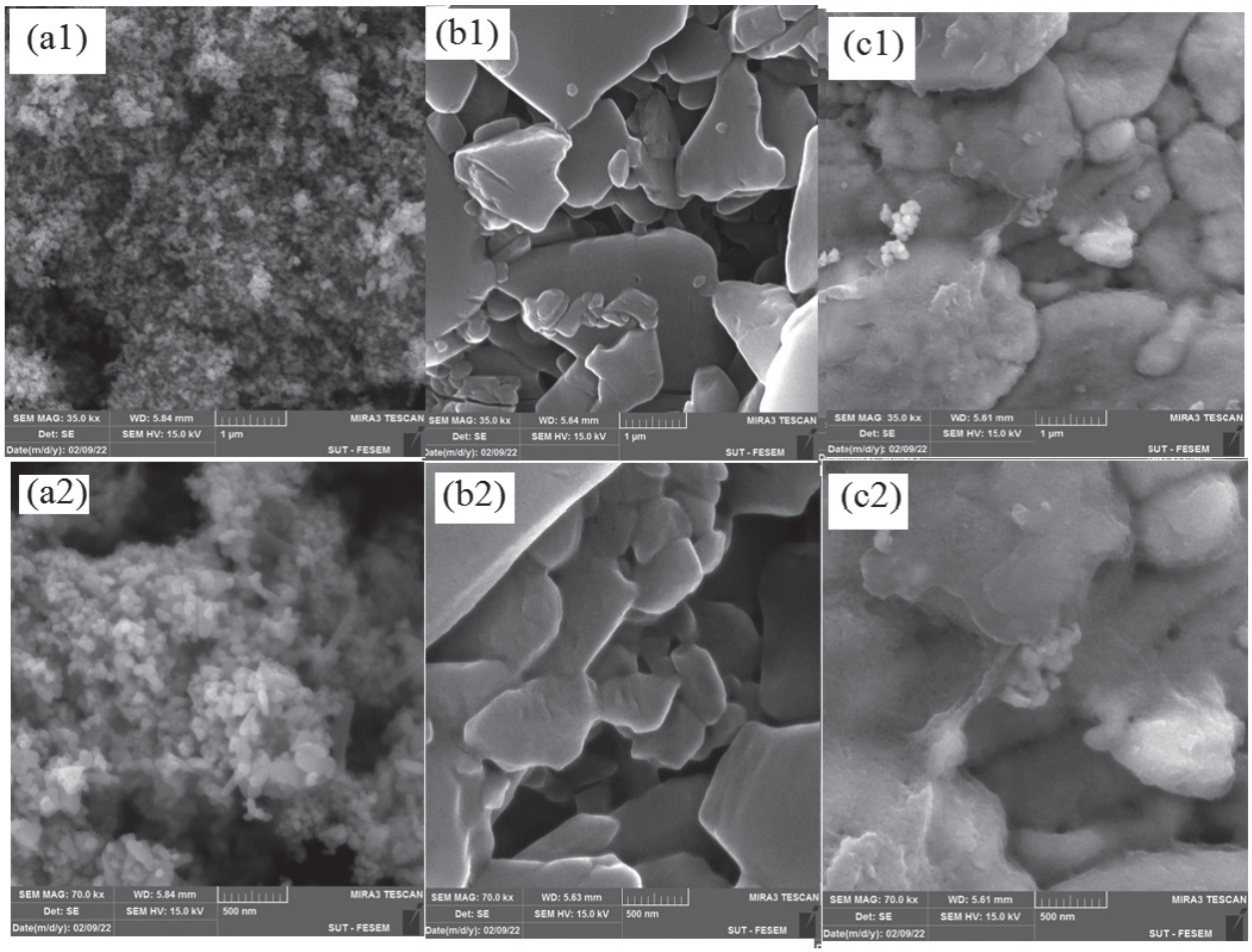

Figure 6. SEM micro images of (**a**) ZnO-HNPs, (**b**) metronidazole, (**c**) metronidazole-ZnO-HNPs, (1)1 µm, and (2)500 µm.

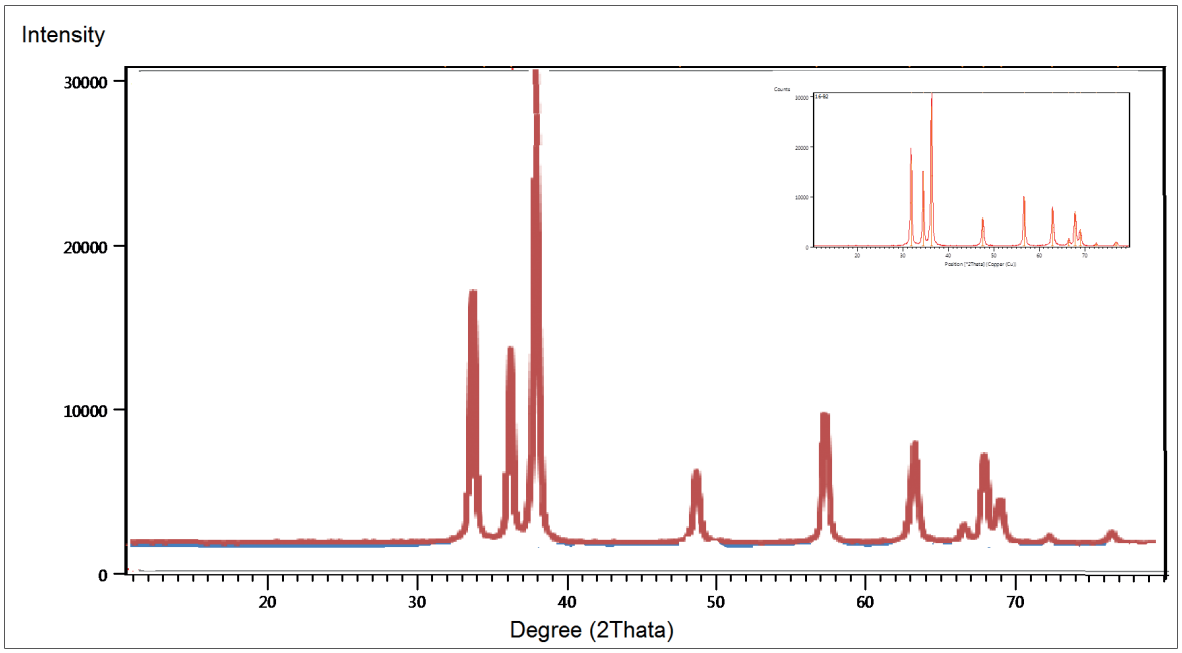

Figure 7. X-ray diffraction of the synthesized ZnO-HNPs.

554 cm^{-1} is a characteristic band of the pure "ZnO wurtzite hexagon phase" (Bitenc et al. 2009). The absorption peaks at 3250 and 3400 cm^{-1} are correspond to hydroxyl (OH) groups, The stretching vibration of C=O is observed at 1400–1600 cm^{-1}. Also, the absorption peaks at 1400, 1560, 2900, and 2980 cm^{-1} are correlated with both symmetric and asymmetric extending vibrations for CH_2 and CH_3 groups together.

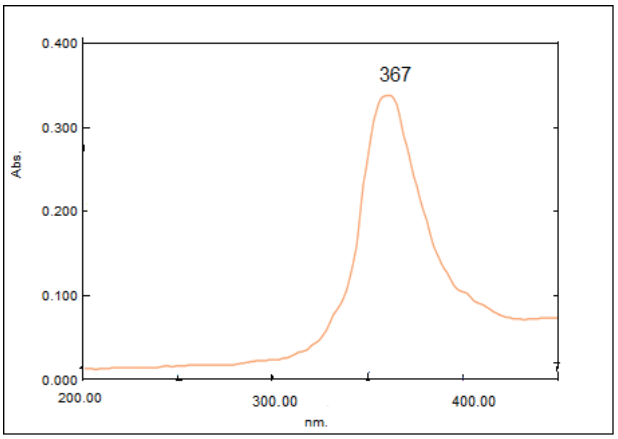

Figure 8. UV-visible spectrophotometric absorbance spectrum for ZnO-HNPs.

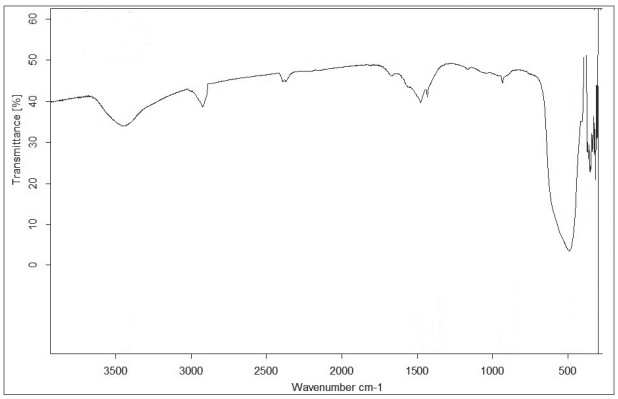

Figure 9. Fourier transform infrared spectroscopy for functionalization of ZnO-HNPs.

Fig. 10 shows the FTIR spectra of metronidazole, ZnO-NPs, and nano-loaded metronidazole/ZnO. The absorption bands (3622 cm^{-1} and 3437 cm^{-1}) represent the metronidazole O-H groups (Khataee et al. 2016). The widespread adsorption bands seen between 3050 and 3600 cm^{-1} are correlated with the stretching vibrations of the OH group. As well, the adsorption peaks of 600 cm^{-1}, 1050 cm^{-1}, and 1610 cm^{-1} are associated with the bending vibration of C-H, besides the stretching vibrations of C=O and C=C, respectively. The functional groups at 720 cm^{-1}, 1490 cm^{-1}, 1710 cm^{-1}, and 2980 cm^{-1} are corresponded to the stretching vibration of ZnO. The FTIR spectrum of ZnO-HNPs (Fig. 10a) displays the peak at 424 cm^{-1}, which is due to the stretching vibration of Zn-O (PP 2020). Distinctive peaks of metronidazole and zinc oxide observed in Fig. 10c, confirm the effective formation of loaded ZnO-NPs-metronidazole (Nasseh et al. 2020).

Fig. 11a, b, and c represent the FTIR spectra of the synthesized ZnO-NPs, clindamycin, and clindamycin/ZnO-NPs, which are obtained at spectra of 4000–400 cm^{-1}. The ZnO-NPs spectrum with the bands for the active groups situated at "[3441, 3105, 1611, 1555, 1440, 1392, 1117, 1041, 1019, 693, 950, 946, 624, 620, 568, and 465 cm^{-1}]". The solid wide peaks in the high area at 3441 cm^{-1} and 3105 cm^{-1} are attributed to the stretching vibrations of OH groups (Vaishnav et al. 2017). Absorption peaks at 1611

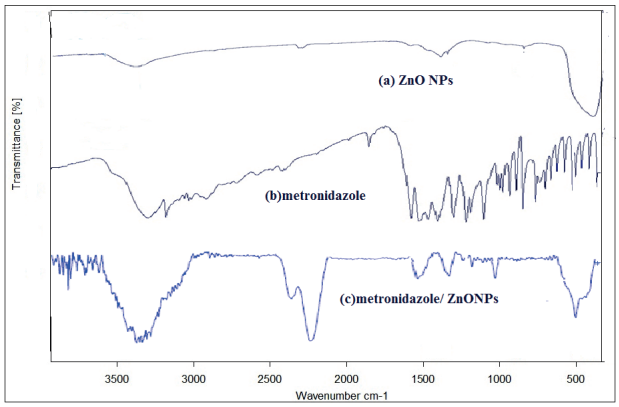

Figure 10. Fourier transform infrared spectroscopy for functionalization of (**a**) hexagonal ZnO-NPs, (**b**) metronidazole, and (**c**).

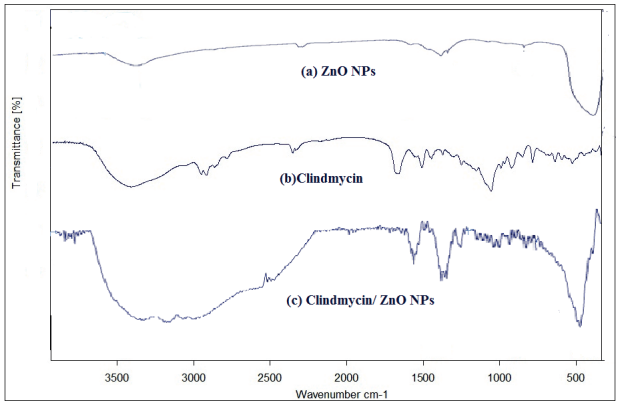

Figure 11. The FTIR for functionalization of (**a**) ZnO-HNPs, (**b**) clindamycin, and (**c**) loading clindamycin / ZnO-HNPs.

and 1555 cm^{-1} are attributed to the C=O amide I and II groups. The bending vibration band of –C–H gets up at 1440 and 1392 cm^{-1}. Peaks at 1117, 1041, and 1019 cm^{-1}, correspond to C–O stretching vibration, while that at 950, 946, and 693 cm^{-1} correspond to =C–H bending vibration. Whereas, the bending vibration of O–H group appear at 624 and 620 cm^{-1}. Both the 568 and 465 cm^{-1} peaks are due to Zn–O stretching vibration which confirms the synthesis of the desired product. We performed the FTIR analysis to detect the probable molecules cause the bio-reduction of ZnO-NPs (34).

3.2. Antibacterial activity of ZnO-HNPs

Figs 12 and 13 illustrate the antibacterial effect of ZnO-HNPs which was measured by the "agar well diffusion" technique against bacterial pathogens including both gram-negative (*Pseudomonas aeruginosa*) and gram-positive (*Staphylococcus aureus*). The inhibition zone calculated in mm.

The antibacterial activity of ZnO-HNPs was measured in triplicate (1, 0.5, and 0.1%) toward gram-positive and gram-negative bacteria using the "agar well diffusion technique" as we can see in Figs 12, 13 and Tables 1, 2. The Staphylococcus aureus showed more sensitivity to ZnO-HNPs (0.1%) in the 12 mm inhibition zone, while ZnO-HNPs (0.5%) exhibited the least sensitivity in the 10 mm inhibition zone. Our result was also consistent with

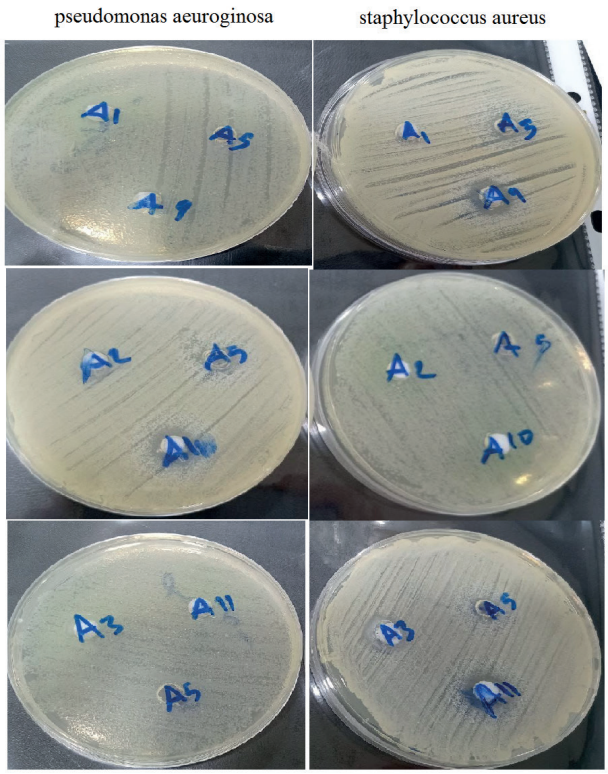

Figure 12. Antibacterial activity of ZnO-HNPs: (A1=1%), (A2=0.5%), (A3=0.1%), metronidazole (A5), and metronidazole / ZnO-HNPs (A9= metronidazole /1% ZnO-HNPs), (A10= metronidazole /0.5%ZnO HNPs), (A9= metronidazole /0.1%ZnO-HNPs).

Table 1. The diameter of ZnO-HNPs inhibition zone of metronidazole, and metronidazole/ZnO-HNPs against S. aureus and *P. aeruginosa* bacteria.

Sample	Diameter of inhibition zone (mm)	
	Staphylococcus aureus	*Pseudomonas aeruginosa*
A1	0	0
A2	10	0
A3	12	0
A5	15	0
A9	20	0
A10	25	0
A11	20	0

the finding of Premanathan et al. (2011), Raghupathi et al. (2011), and Safawo et al. (2018).

Antibacterial action of ZnO-HNPs was examined against *Pseudomonas aeruginosa* and *S. aureus* bacterial strains. Drug loaded ZnO-HNPs were shown to be more active against *S. aureus* (Figs 12, 13). The activity of ZnO-HNPs was increased after mixing with various concentrations of metronidazole or clindamycin. However, no response observed against bacterial strain of Pseudomonas aeruginosa. The inhibition zones formed in the antibacterial screening tests specified that the synthesized ZnO-NPs have antibacterial activity toward pathogenic bacteria. The synthesized ZnO-HNPs might be of enormous use in medicine for this effective antibacterial activity (Khataee et al. 2016; Thamer et al. 2021).

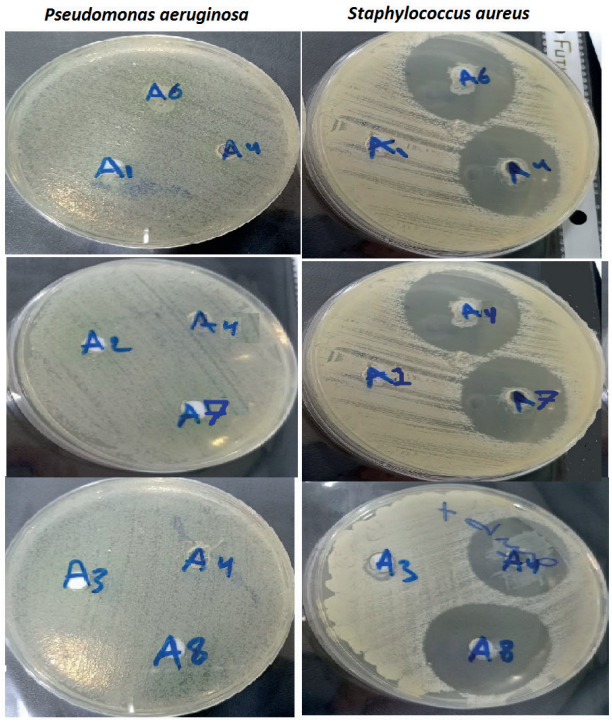

Figure 13. Antibacterial activity of ZnO-HNPs: (A1=1%), (A2=0.5%), (A3=0.1%), clindamycin (A4), and clindamycin/ ZnO-NPs (A6= clindamycin /1% ZnO-HNPs), (A7= clindamycin /0.5%ZnO-HNPs), (A8= clindamycin /0.1% ZnO-HNPs).

Table 2. Diameter of inhibition zone by ZnO-HNPs, clindamycin, and clindamycin /ZnO-HNPs against *Staphylococcus aureus*, and *Pseudomonas* aeruginosa.

Sample	diameter inhibition Zone in mm	
	Staphylococcus aureus	*Pseudomonas aeruginosa*
A1	0	0
A2	10	0
A3	12	0
A4	15	0
A6	30	0
A7	35	0
A8	38	0

The possible mechanism of the ZnO-NP antibacterial activity depends on the rough external texture of ZnO-HNPs that bind with the bacterial exterior because of the electric forces, which kill bacteria directly. Smaller particulate size offers quite greater surface area and high quantity of Zn atoms that induce toxic effects of ZnO against the bacteria as shown in Fig. 1 . The outcomes of the clindamycin /ZnO-HNPs were similar to that with metronidazole/ZnO-HNPs. Clindamycin/ZnO-HNPs had exposed superior results than metronidazole/ZnO-HNPs toward *P. aeruginosa* (Khataee et al. 2016).

Bacterial resistance is a foremost issue that remains a difficulty in all healthcare systems of developing and developed nations. Recent bacterial treatment has been affected by the increase and propagation of multidrug-resistant pathogens. The use of plant-mediated nanomaterials as a

new source of antimicrobials was considered since they have a diversity of active mixtures with proven beneficial features (Romero et al. 2005; Faisal et al. 2021).

In the current study, green synthesis approaches for producing metallic NPs have become a valuable development. The usage of phytochemicals from plant extract has become more popular in NPs synthesis, owing to the dual advantages of phytochemicals as reducing and capping agents to the NPs. Zinc oxide NPs in the current study were produced from a common medicinal plant and their antibacterial activity was measured against gram-positive and negative strains.

Conclusion

The green precipitation technique was utilized for the synthesis of ZnO-HNPs using fresh "*Ziziphus* leaf extract" from local gardens. Results from X-ray diffraction indicate the formation of high crystallinity hexagonal ZnO nanostructure. The actual mean size distribution of NPs was 44.63 nm as measured by SEM.

Various ZnO-HNP formulations have been developed as an alternative drug delivery approach to treat bacterial infections. Hence, ZnO-HNPs can be utilized for the controlled delivery of clindamycin or metronidazole. The current study was performed on both gram-positive and negative bacteria and the antibacterial activity increases with increased drug loading. The diameter of the inhibition zone by loading clindamycin/ZnO-HNPs was 30, 35, and 38 mm. While the diameter of the inhibition zone by loading metronidazole/ZnO- HNPs was 20, and 25 mm. The antibacterial efficacy of clindamycin or metronidazole-loaded ZnO-HNPs was non significant against *P. aeruginosa*.

References

Abdelraheem WM, Khairy RM, Zaki AI, Zaki SH (2021) Effect of ZnO nanoparticles on methicillin, vancomycin, linezolid resistance and biofilm formation in *Staphylococcus aureus* isolates. Annals of Clinical Microbiology and Antimicrobials 20(1): 1–11. https://doi.org/10.1186/s12941-021-00459-2

Abd EL-Tawab A, Abo El-Roos N, El-Gendy AAM, Abd EL-Tawab (2018) Effect of zinc oxide nanoparticles on *Staphylococcus aureus* isolated from cows'mastitic milk. Benha Veterinary Medical Journal 35(1): 30–41. https://doi.org/10.21608/bvmj.2018.35946

Ada K, Gökgöz M, Önal M, Sarıkaya Y (2008) Preparation and characterization of a ZnO powder with the hexagonal plate particles. Powder Technology 181(3): 285–291. https://doi.org/10.1016/j.powtec.2007.05.015

Ahmed S, Chaudhry SA, Ikram S (2017) A review on biogenic synthesis of ZnO nanoparticles using plant extracts and microbes: A prospect towards green chemistry. Journal of Photochemistry and Photobiology B: Biology 166: 272–284. https://doi.org/10.1016/j.jphotobiol.2016.12.011

Alnehia A, Al-Hammadi AH, Al-Sharabi A, Alnahari H (2022) Optical, structural and morphological properties of ZnO and Fe+ 3 doped ZnO-NPs prepared by *Foeniculum vulgare* extract as capping agent for optoelectronic applications. Inorganic Chemistry Communications 143: 109699. https://doi.org/10.1016/j.inoche.2022.109699

Arif M, Ullah R, Ahmad M, Ali A, Ullah Z, Ali M, Al-Joufi FA, Zahoor M, Sher H (2022) Green synthesis of silver nanoparticles using *Euphorbia wallichii* leaf extract: Its antibacterial action against citrus canker causal agent and antioxidant potential. Molecules 27(11): 3525. https://doi.org/10.3390/molecules27113525

Bitenc M, Orel ZC (2009) Synthesis and characterization of crystalline hexagonal bipods of zinc oxide. Materials Research Bulletin 44(2): 381–387. https://doi.org/10.1016/j.materresbull.2008.05.005

Bitenc M, Drazic G, Orel ZC (2010) Characterization of crystalline zinc oxide in the form of hexagonal bipods. Crystal Growth & Design 10(2): 830–837. https://doi.org/10.1021/cg901193g

Chikkanna MM, Neelagund SE, Rajashekarappa KK (2019) Green synthesis of zinc oxide nanoparticles (ZnO NPs) and their biological activity. SN Applied Sciences 1(1): 1–10. https://doi.org/10.1007/s42452-018-0095-7

da Silva BL, Abuçafy MP, Manaia EB, Junior JAO, Chiari-Andréo BG, Pietro RCR, Chiavacci LA (2019) Relationship between structure and antimicrobial activity of zinc oxide nanoparticles: An overview. International Journal of Nanomedicine 14: 9395–9410. https://doi.org/10.2147/IJN.S216204

Dhanalekshmi UM, Alam T, Khan SA (2022) The Folkloric Uses and Economic Importance of Some Selected Edible Medicinal Plants Native to Oman: A Brief Overview. Edible Plants in Health and Diseases, 29 pp. https://doi.org/10.1007/978-981-16-4880-9_1

Faisal S, Jan H, Shah SA, Shah S, Khan A, Akbar MT, Rizwan M, Jan F, Wajidullah, Akhtar N, Khattak A, Syed S (2021) Green synthesis of zinc oxide (ZnO) nanoparticles using aqueous fruit extracts of *Myristica fragrans*: Their characterizations and biological and environmental applications. ACS Omega 6(14): 9709–9722. https://doi.org/10.1021/acsomega.1c00310

Haque M, Sartelli M, McKimm J, Bakar MA (2018) Health care-associated infections–an overview. Infection and Drug Resistance 11: 2321–2333. https://doi.org/10.2147/IDR.S177247

Hammadi AH, Habeeb SA, Al-Jibouri LF, Hussien FH (2020) Synthesis, Characterization and Biological Activity of Zinc Oxide Nanoparticles (ZnO NPs). Systematic Reviews in Pharmacy 11(5): 431–439.

Jamdagni P, Khatri P, Rana JS (2016) Nanoparticles based DNA conjugates for detection of pathogenic microorganisms. International Nano Letters 6(3): 139–146. https://doi.org/10.1007/s40089-015-0177-0

Khataee A, Kiranşan M, Karaca S, Arefi-Oskoui S (2016) Preparation and characterization of ZnO/MMT nanocomposite for photocatalytic ozonation of a disperse dye. Turkish Journal of Chemistry 40(4): 546–564. https://doi.org/10.3906/kim-1507-77

Kolekar TV, Bandgar SS, Shirguppikar SS, Ganachari VS (2013) Synthesis and characterization of ZnO nanoparticles for efficient gas sensors. Archives of Applied Science Research 5(6): 20–28.

Kung JC, Wang WH, Lee CL, Hsieh HC, Shih CJ (2020) Antibacterial activity of silver nanoparticles (AgNP) confined to mesostructured,

silica-based calcium phosphate against methicillin-resistant *Staphylococcus aureus* (MRSA). Nanomaterials 10(7): 1264. https://doi.org/10.3390/nano10071264

Malode SJ, Keerthi PK, Shetti NP, Kulkarni RM (2020) Electroanalysis of carbendazim using MWCNT/Ca-ZnO modified electrode. Electroanalysis 32(7): 1590–1599. https://doi.org/10.1002/elan.201900776

Matussin S, Harunsani MH, Tan AL, Khan MM (2020) Plant-extract-mediated SnO2 nanoparticles: Synthesis and applications. ACS Sustainable Chemistry & Engineering 8(8): 3040–3054. https://doi.org/10.1021/acssuschemeng.9b06398

Mohamed MF, Abdelkhalek A, Seleem MN (2016) Evaluation of short synthetic antimicrobial peptides for treatment of drug-resistant and intracellular *Staphylococcus aureus*. Scientific Reports 6(1): 1–14. https://doi.org/10.1038/srep29707

Moghri MM, Borghei SM, Taleshi F (2012) Synthesis and characterization of nano-sized hexagonal and spherical nanoparticles of zinc oxide.

Nasseh N, Arghavan FS, Rodriguez-Couto S, Panahi AH, Esmati M (2020) Preparation of activated carbon@ZnO composite and its application as a novel catalyst in catalytic ozonation process for metronidazole degradation. Advanced Powder Technology 31(2): 875–885. https://doi.org/10.1016/j.apt.2019.12.006

Palanikumar L, Ramasamy S, Hariharan G, Balachandran C (2013) Influence of particle size of nano zinc oxide on the controlled delivery of Amoxicillin. Applied Nanoscience 3(5): 441–451. https://doi.org/10.1007/s13204-012-0141-5

Perveen R, Shujaat S, Qureshi Z, Nawaz S, Khan MI, Iqbal M (2020) Green versus sol-gel synthesis of ZnO nanoparticles and antimicrobial activity evaluation against panel of pathogens. Journal of Materials Research and Technology 9(4): 7817–7827. https://doi.org/10.1016/j.jmrt.2020.05.004

Peterson E, Kaur P (2018) Antibiotic resistance mechanisms in bacteria: Relationships between resistance determinants of antibiotic producers, environmental bacteria, and clinical pathogens. Frontiers in Microbiology 9: 2928. https://doi.org/10.3389/fmicb.2018.02928

Mahalakshmi S, Hema N, Vijaya PP (2020) In vitro biocompatibility and antimicrobial activities of zinc oxide nanoparticles (ZnO NPs) prepared by chemical and green synthetic route—A comparative study. BioNanoScience 10(1): 112–121. https://doi.org/10.1007/s12668-019-00698-w

Premanathan M, Karthikeyan K, Jeyasubramanian K, Manivannan G (2011) Selective toxicity of ZnO nanoparticles toward Gram-positive bacteria and cancer cells by apoptosis through lipid peroxidation. Nanomedicine; Nanotechnology, Biology, and Medicine 7(2): 184–192. https://doi.org/10.1016/j.nano.2010.10.001

Qureshi K, Ahmad MZ, Bhatti IA, Zahid M, Nisar J, Iqbal M (2019) Graphene oxide decorated ZnWO4 architecture synthesis, characterization and photocatalytic activity evaluation. Journal of Molecular Liquids 285: 778–789. https://doi.org/10.1016/j.molliq.2019.04.139

Raghupathi KR, Koodali RT, Manna AC (2011) Size-dependent bacterial growth inhibition and mechanism of antibacterial activity of zinc oxide nanoparticles. Langmuir 27(7): 4020–4028. https://doi.org/10.1021/la104825u

Rahman A, Harunsani MH, Tan AL, Khan MM (2021) Zinc oxide and zinc oxide-based nanostructures: Biogenic and phytogenic synthesis, properties and applications. Bioprocess and Biosystems Engineering 44(7): 1333–1372. https://doi.org/10.1007/s00449-021-02530-w

Roy A, Gauri SS, Bhattacharya M, Bhattacharya J (2013) Antimicrobial activity of CaO nanoparticles. Journal of Biomedical Nanotechnology 9(9): 1570–1578. https://doi.org/10.1166/jbn.2013.1681

Rizzello L, Pompa PP (2014) Nanosilver-based antibacterial drugs and devices: Mechanisms, methodological drawbacks, and guidelines. Chemical Society Reviews 43(5): 1501–1518. https://doi.org/10.1039/C3CS60218D

Romero CD, Chopin SF, Buck G, Martinez E, Garcia M, Bixby L (2005) Antibacterial properties of common herbal remedies of the southwest. Journal of Ethnopharmacology 99(2): 253–257. https://doi.org/10.1016/j.jep.2005.02.028

Safawo T, Sandeep BV, Pola S, Tadesse A (2018) Synthesis and characterization of zinc oxide nanoparticles using tuber extract of anchote (*Coccinia abyssinica* (Lam.) Cong.) for antimicrobial and antioxidant activity assessment. OpenNano 3: 56–63. https://doi.org/10.1016/j.onano.2018.08.001

Scherrer P (1918) Nachrichten von der Gesellschaft der Wissenschaften zu Göttingen. Mathematisch-Physikalische Klasse 2: 98–100.

Siddiqi KS, Husen A, Rao RA (2018) A review on biosynthesis of silver nanoparticles and their biocidal properties. Journal of Nanobiotechnology 16(1): 1–28. https://doi.org/10.1186/s12951-018-0334-5

Sornalatha DJ, Murugakoothan P (2014) Characterization of hexagonal ZnO nanostructures prepared by hexamethylenetetramine (HMTA) assisted wet chemical method. Materials Letters 124: 219–222. https://doi.org/10.1016/j.matlet.2014.03.100

Thamer R, Alsammak E (2021) Synergistic effect of Zinc Oxide nanoparticles and Vancomycin on Methicillin resistant *Staphylococcus aureus*. Journal of Life and Bio Sciences Research 2(01): 01–06. https://doi.org/10.38094/jlbsr1332

Tong SY, Davis JS, Eichenberger E, Holland TL, Fowler Jr VG (2015) *Staphylococcus aureus* infections: Epidemiology, pathophysiology, clinical manifestations, and management. Clinical Microbiology Reviews 28(3): 603–661. https://doi.org/10.1128/CMR.00134-14

Vadekeetil A, Chhibber S, Harjai K (2019) Efficacy of intravesical targeting of novel quorum sensing inhibitor nanoparticles against *Pseudomonas aeruginosa* biofilm-associated murine pyelonephritis. Journal of Drug Targeting 27(9): 995–1003. https://doi.org/10.1080/1061186X.2019.1574802

Vaishnav J, Subha V, Kirubanandan S, Arulmozhi M, Renganathan S (2017) Green synthesis of zinc oxide nanoparticles by *Celosia argentea* and its characterization. Journal of Optoelectronic and Biomedical Materials 9: 59–71.

Vijayakumar S, Krishnakumar C, Arulmozhi P, Mahadevan S, Parameswari N (2018) Biosynthesis, characterization and antimicrobial activities of zinc oxide nanoparticles from leaf extract of *Glycosmis pentaphylla* (Retz.) DC. Microbial Pathogenesis 116: 44–48. https://doi.org/10.1016/j.micpath.2018.01.003

Zoubir J, Radaa C, Bougdour N, Idlahcen A, Bakas I, Assabbane A (2021) Electro-detection of the antibacterial metronidazole using zinc oxide nanoparticles formed on graphitic carbon sheets. Analytical application: Human serum and urine. Materials Science for Energy Technologies 4: 177–188. https://doi.org/10.1016/j.mset.2021.06.001